Thermodynamic and Economic Optimization of a Solar-powered Stirling engine for Micro-Cogeneration Purposes

Ana C. Ferreira[a], Manuel L. Nunes[a], José C. Teixeira[b], Luís B. Martins[b] and Senhorinha F. Teixeira[a]

[a] Department of Production and Systems, School of Engineering, University of Minho, Azurém Campus, 4800-058 Guimarães, Portugal. {acferreira;lnunes;st}@dps.uminho.pt

[b] Department of Mechanical Engineering, School of Engineering, University of Minho, Azurém Campus, 4800-058 Guimarães, Portugal. {jt;lmartins}@dem.uminho.pt

Abstract:

The micro-CHP systems are a promising technology for improving the energy efficiency of small energy conversion units, located near the end user. The combined heat and power production allows the optimal use of the primary energy sources and provide significant reductions in carbon emissions. Its use, still incipient, has a great potential for applications in the residential sector. This study aims to develop a methodology for the thermal-economic optimization of micro cogeneration units using a Stirling cycle engine as prime mover and concentrated solar energy as the heat source. The analyses were performed through numerical simulations by developing a code in MatLab® programming language, based on the model developed by Urieli and Berchowitz. The mathematical modelling was modified, improved and adapted to adjust the configuration of the Stirling engine for cogeneration applications. The model includes the thermodynamic characterization of the physical model and the definition of purchase cost equation representative of each system component. Each cost equation is based on physical parameters, taking into account the sizing of the system. The maximisation of the annual worth from the system operation was defined as the objective function, subjected to a set of nonlinear thermodynamic and economic constraints in order to give significance to the numerical results. The model was formulated considering a cost/benefit approach, where the terms of the objective function represent a balance between costs and revenues. The decision variables correspond to geometric and operational parameters with the highest relevance in the system operation. The optimization problem was solved by applying the Generalized Pattern Search algorithm. The optimization model was effective in the determination of the optimal solution and a positive annual worth was obtained for the defined input simulation conditions. For the best solution obtained for the micro-CHP system, the economic analysis disclosed a system, economically attractive, with a payback period of approximately 10 years.

Keywords:

Solar-powered Stirling engine; thermal-economic optimization; micro-cogeneration.

1. Introduction

Solar energy can be collected and used to provide electricity or heating and, as a clean energy source, allows the reduction of the fossil fuels consumption and also reduces the environmental impact [1,2]. The direct conversion of solar power into mechanical power reduces both the cost and complexity of the prime mover. Stirling engines are able to use solar energy which is a cheap source of energy [3]. The increasing interest in Stirling engines is largely due to the fact the engine is more environmentally friendly than the widely used technologies. Stirling engines are thermodynamic devices working theoretically on the Stirling cycle and using a compressible fluid as working fluids, such as air, hydrogen, helium or nitrogen. Since the combustion process takes place outside the engine, the continuous combustion process make Stirling engines a smoothly technology, resulting in lower vibration, noise level and emissions when compared with the reciprocating internal combustion engines. This technology is also characterized to have fewer moving parts compared to other engines. Stirling engines have low wear and long maintenance free operating periods [4,5]. Thus, the Stirling engine

offers the possibility for having high efficiency engine with less exhaust emissions when compared with other technologies (e.g. internal combustion engines or micro-gas turbines) [6,7].
More recently, a number of new Stirling engine models have been developed to improve their efficiency and open this technology to new fields of application, namely in micro- and mini-cogeneration systems. Kaushik & Kumar, [8], studied effects of irreversibility of the regenerator and heat transfer process in heat/sink sources. Ust, Sahin & Kodal, [9], introduced a new thermo-economic performance analysis based on an objective function defined as the power output per total cost. Boucher, Lanzetta & Nika, [10], reported a theoretical study of the dynamic behaviour of a dual free-piston Stirling engine coupled with an asynchronous linear alternator. The objective was the evaluation of the thermo-mechanical conditions for a stable operation of the engine. Kongtragool and Wongwises (2006) investigated the effect of regenerator effectiveness and dead volume on the engine network; and the heat input into the engine efficiency by using a theoretical investigation on the thermodynamic analysis of a Stirling engine. Nepveu and his co-authors [11] presented a global thermal model of the energy conversion of the 10 kW_{el} *Eurodish* dish/Stirling unit, using optical measurements to calculate the losses by parabola reflectivity. The authors also performed a thermodynamic analysis of a SOLO Stirling 161 engine. The model was divided in 32 control-volumes and equations of ideal gas, mass and energy conservation are written for each control-volume. The differential equation system was then solved, iteratively by using the MatLab programming environment. Rogdakis *et al.* [5] studied a Solo Stirling Engine V161 cogeneration module via a thermodynamic analysis. Calculations were conducted using different operational conditions concerning the heat load of the engine and the produced electrical power. The authors achieved good results in terms of electrical and thermal efficiencies as well as a positive primary energy saving. Asnaghi and his co-authors [12] also performed a numerical simulation and thermodynamic analysis of a SOLO 161 Solar Stirling engine. He and his co-authors considered several imperfect working conditions, pistons' dead volumes, and work losses in the simulation process. The results indicated that the increase in the heater and cooler temperature difference and the decrease in the dead volumes will lead to an increase in thermal efficiency. Ahmadi and co-authors [13] presented the optimization of a solar-powered high temperature differential Stirling engine considering multiple criteria. A thermal model was developed so that the output power and thermal efficiency of the solar Stirling system with finite rate of heat transfer, regenerative heat loss, conductive thermal bridging loss, finite regeneration process time and imperfect performance of the dish collector could be obtained. The solar absorber temperature and the highest and lowest temperatures of the working fluid were considered as decision variables.
This study aims to develop a methodology for the thermodynamic and economic optimization of micro-cogeneration unit using a Stirling cycle engine as prime mover and concentrated solar energy as the heat source. A detailed thermodynamic study was carried out to define the model for the physical characterization of the Stirling engine, including the limitations in the heat transfer processes and losses due to pumping effects. The heat costs from the solar energy source were also included in the model. The economic model is also presented and a purchase cost equation was developed to estimate the total system investment cost. Both thermodynamic and economic were coded in MatLab programming language and an optimization algorithm was applied. Eight decision variables were selected and the maximisation of the annual worth was defined as the objective function.

2. System description

This study is focused on the optimization of a micro-CHP system based on a Stirling engine as prime mover, able to produce 1-5 kW_{el} of electricity and a larger heat load (3-17.5 kW_{th}). These values of energy output are suitable to fulfil most of the energy requirements of a residential dwelling.
Accordingly to the literature [14], the micro-CHP systems based on Stirling engine technology for this scale of application, have a thermal power output in a range of 2-35 kW_{th}. The Stirling engine consists of an engine piston (small tightly sealed piston that moves out when the gas inside the engine expands), the exchanger piston (a larger piston that moves easily between the heated and cooled sections of the engine) and three heat exchangers: a heater, a regenerator and a cooler. The engine piston converts the pressure variation of the working gas into mechanical power, whereas the exchanger piston is used to move the working gas between the hot and cold sources. Considering the forms of cylinder coupling,

these engines can be classified in three arrangements: alpha, beta and gamma. In this research, the alpha-Stirling configuration was chosen to be modelled. The working gas flows between these two spaces by alternate crossing of, a low temperature heat exchanger (cooler), a regenerator and a high temperature heat source (heater), connected in series. Thus, the Stirling configuration (Figure 1) is considered as a set of five connected components: compression space (*c*), cooler (*k*), regenerator (*r*), heater (*h*) and expansion space (*e*). Each engine component represents an entity endowed with its respective volume (*V*), temperature (*T*), absolute pressure (*P*), mass (*m*), as a function of crank angle.

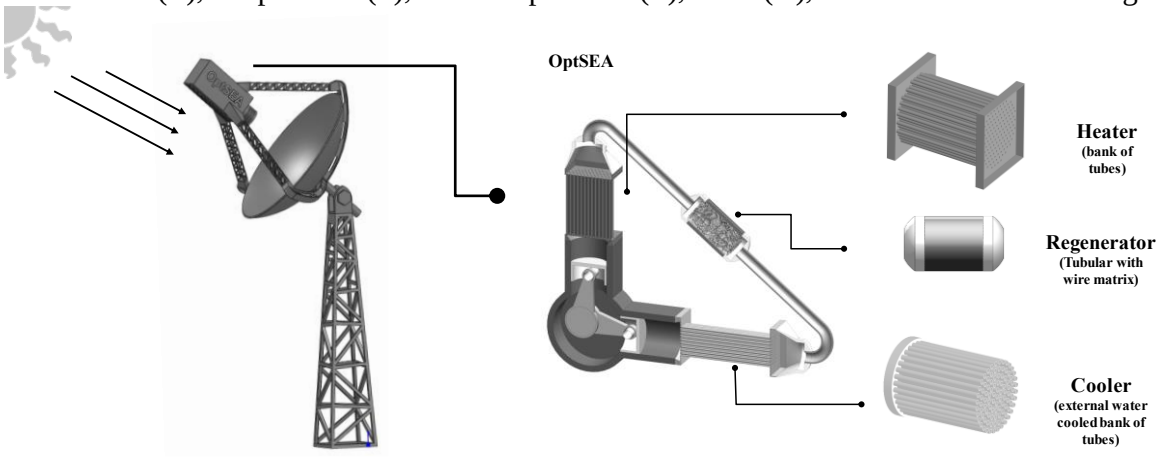

Fig. 1. Schematic layout of solar-powered Stirling engine for micro-cogeneration.

Heat is transferred from the external heat source to the working gas in the heater, cyclically stored and recovered in the regenerator, and rejected by the working gas in the cooler. Thus, the working gas temperature varies between two values: the hot source from the parabolic solar dish and cold sink temperature. The cold sink of the engine is a mass flow of water that removes heat from the cooler to produce hot water. It was assumed that the mass flow of water is heated from 288 K to 343 K.

3. Mathematical Model

3.1. Objective Function

The objective function of this optimization model is defined as the maximisation of the Annual Worth (*AW*) of the power plant. It represents the balance between the incomes and the costs of the system operation, as described in (1).

$$\begin{aligned} &max\ AW \\ &where \quad AW = R_{sell} + C_{avoided} + R_{res} - C_{inv} - C_m \end{aligned} \tag{1}$$

The revenues are: the income from selling electricity to the grid (R_{sell}), the residual value of the system at its lifetime end (R_{res}) and the avoided cost of heat generation by a conventional boiler ($C_{avoided}$). The costs considered were: the annual system investment cost (C_{inv}) and the maintenance costs involved in the production of electricity and heat using the CHP system (C_m). The annual income from selling electricity power to the grid was calculated from the electrical power delivered to the grid ($\dot{W}_{el}$) considering the yearly number of system working yours (t) which corresponds to 3000 h, multiplied by the electricity-selling price (p_{sell}), as in (2).

$$R_{\text{sell}} = \dot{W}_{el} \cdot p_{\text{sell}} \cdot t \tag{2}$$

The electricity-selling price was taken as a guaranteed and fixed Feed-In-Tariff (FIT) of 0.12 EUR/kWh. The avoided cost represents the cost of Natural Gas (NG) that would be consumed by a conventional system (typically a boiler) to produce the same amount of useful thermal energy, *Q*. This avoided cost can be calculated as in (3).

$$\text{C}_{\text{avoided}} = p_{\text{fuel}} \cdot \frac{Q}{\eta_b} \tag{3}$$

where, p_{fuel}, is the NG price per energy unit (p_{fuel}=10 EUR/GJ) on a Low Heating Value (LHV) basis and η_b is the efficiency of a conventional boiler. This value is usually assumed to be 90%.

The annual system investment cost, $C_{inv,}$ is calculated according to the annualised capital cost. Annualising the initial investment corresponds to the spreading of the initial cost across the lifetime of a system, while accounting for the time value of the money. The initial capital cost is annualised as if it was being paid off a loan at a particular interest of discount rate over the lifetime of the option. The power production costs are sensitive to changes in the discount rate (i.e. the interest rate used to determine the present value of future cash flows). The Capital Recovery Factor (CRF) is used to determine the equal amounts of cash transactions for an investment and can be expressed as in (4).

$$CRF = \frac{i_e(1+i_e)^n}{(1+i_e)^n - 1} \tag{4}$$

where i_e is the effective rate of return, and n is the estimated number of years of the system lifetime. The lifetime of the system was defined to be 20 years. According to [15], the total accumulated operating time for the Stirling engines is about 180000 h, corresponding to ≅ 20.5 years. In addition, some caution should be taken when a new technology is applied to an emergent market, and so, the investment risks are higher than with mature technologies and traditional markets.

For thermal-economic optimisation, the i_e can be approximated as: nominal rate of return (interest rate) minus inflation rate plus owners' risk factor and correction for the method of compounding. The i_e herein considered was 7%, resulting in a CRF of 0.0944. Thus, the annual system investment cost becomes as in (5).

$$C_{inv} = \sum_i C_i \cdot CRF \tag{5}$$

where C_i is the purchase cost of each component of the CHP system ($C_i \rightarrow C_k$; C_h; C_r; C_{eng}; $C_{solardish}$). The purchase cost equations are presented in the next subsection. For Stirling engines, the normal maintenance intervals are of 5000-8000 h. According to a Swedish study [15], the maintenance service can include the regenerator maintenance and the replacement of some engine components, oil and filters. The total maintenance costs are estimated to be 0.015 EUR/kWh$_{el}$. Thus, the maintenance costs, C_m, are evaluated as in (6).

$$C_m = p_m \cdot \dot{W}_{el} \cdot t \tag{6}$$

where p_m is the maintenance price per unit of electricity produced (0.015 EUR/kW$_{el}$). The electrical power ($\dot{W}_{el}$) already accounts for the efficiency of the electrical generator, herein assumed to be 93%. The residual value of equipment was estimated as a percentage (ψ) of the C_{inv}, of about 5%.

3.2. Purchase Cost Equations

Five purchase cost equations were defined in order to estimate the cost of the thermal plant. The mathematical expressions that define the purchase cost of each component were based on the methodology developed by Marechal *et al.* [16]. The costing methodology consists on the derivation of an expression for each component by integrating thermodynamic and cost coefficients, adjusted for this kind of technology, and also taking into account real market data. Each cost equation was defined considering physical variables, which can be classified as size and quality variables. As a result of this thermodynamic integrated model, the cost estimation can be performed in order to evaluate the overall cost of the system for a specific range of combined power production. In terms of methodology, the equations were defined considering that the cost of each component is based on a reference case and includes a cost coefficient (in €/K.m^2), a factor of size (dimensionless), which scales the component, and a temperature quality factor (in K). For the heater, regenerator and cooler, the equations relate the cost of the exchanger with its effective heat transfer area $A_{w,h}$, $A_{w,r}$, $A_{w,k}$, respectively (in m^2). Considering the range of the working fluid temperatures reached at the heater and the regenerator, their costs are constrained in terms of materials used in their manufacture. As a consequence, the cost of these two heat exchangers is adjusted considering a temperature quality factor (see (7) and(8)). All the cost coefficients were estimated considering a reference case from a system available in the market [17].

$$C_h = C_{11,h} A_{ref\ w,h} \left(\frac{A_{w,h}}{A_{ref\ w,h}} \right)^{0.5} \left[\frac{1 + e^{C_{12,h} \cdot (T_h - 725)}}{2} \right] \tag{7}$$

$$C_r = C_{21,r} A_{ref\ w,r} \left(\frac{A_{w,r}}{A_{ref\ w,r}} \right)^{0.6} \left[\frac{1 + e^{C_{22,r} \cdot (T_r - 600)}}{2} \right] \quad (8)$$

The cooler was defined as a bundle of parallel tubes, exchanging heat with the working fluid in the internal side and with a mass flow of water on the outside. The gas flow conditions in the cooler are similar to the heater but at a lower temperature. Therefore, in defining the cooler purchase cost, the temperature correction factor was not considered. The cooler purchase cost equation is presented by (9).

$$C_k = C_{31,k} A_{ref\ w,k} \left(\frac{A_{w,k}}{A_{ref\ w,k}} \right)^{0.4} \quad (9)$$

The power of Stirling engines is affected by changing the operational parameters such as the pressure, phase angle, volume and speed. For the engine bulk, it was assumed that there are two main variables that affect the engine cost: the cylinders volumes (V_{eng}, in cm^3), a size factor, and the mean operation pressure (P_{mean}, in bar), which influences the cost of sealants. This purchase cost is representative of both the compression and expansion engine cylinders and it is defined in (10).

$$C_{eng} = C_{41,eng} \left[V_{ref,eng} \left(\frac{V_{eng}}{V_{ref,eng}} \right)^{0.35} \right] \cdot \left[P_{ref,mean} \left(\frac{P_{mean}}{P_{ref,mean}} \right)^{0.2} \right] \quad (10)$$

There is a significant variation on costs for different sizing parameters. Its choice must take into account the application and the power output of the thermal engine. In order to calculate these physical variables and parameters, the physical thermodynamic model has to be defined.

A sun-tracking concentrating collector is a special energy exchanger that converts absorbed solar irradiation in energy which is then transferred to working fluid. A sun-tracking concentrating dish usually has concave reflecting surfaces to intercept and focus the solar irradiation to a much smaller receiving area, resulting in an increased heat flux so that the thermodynamic cycle can achieve higher Carnot efficiency when working at higher temperatures. For the parabolic dish concentrator, it was assumed that there are two main variables that affect the its cost: the dish area, $A_{solardish}$, and the efficiency of the parabolic dish concentrator, $\eta_{collection}$, as in (11),

$$C_{solardish} = C_{fix} + C_{51} \cdot A_{ref,\ solardish} \cdot \left(\frac{A_{solardish}}{A_{ref,\ solardish}} \right)^{0.7} \cdot \eta_{collection} \quad (11)$$

The efficiency of the parabolic dish concentrator can be calculated through the most significant parameters, their concentration ratios. Therefore, the parabolic dish efficiency can be calculated as the ratio between the rate of flow concentration and the geometric concentration ratio. The purchase cost of this component also includes the costs of a commercial sun tracking system (ETATRACK Active 400) as well as the inverter (AJ- 600-24 V), and the engineering costs represent a fix cost, C_{fix}. The reference cost coefficient in (11) was determined considering the purchase prices for *EuroDish*© system, conveniently calculated for the European market [17].

3.3. Physical Model

3.3.1. Stirling Engine

The physical mathematical model integrates an iterative process in order to reach the numerical solution for the thermodynamic cycle. It invokes an Ideal Adiabatic simulation and, sequentially a Non-ideal simulation that evaluates the heat transfer and pressure loss effects in the Stirling engine. In the Ideal Adiabatic analysis, the model is treated as a "*quasi steady-flow*" system. A set of ordinary differential equations is iteratively solved, considering an initial-value problem in which all the variables are arbitrated and the equations are integrated from that initial state over a complete cycle. The final state of the cycle is then used as a new initial-value for a new cycle and several iterations are made until cycle convergence is obtained. The resulting equations are linked by applying the mass and energy equations across the entire system. Enthalpy is transported by means of mass flow and temperature entering and/or

exiting at each component. Each component of the Stirling engine is considered as a single cell (i.e. with uniform properties) where a working fluid mass flow suffers compression and expansion. The derivative operator is denoted by *d*, thus for example *dm* refers to the mass derivative as a function of the cycle crank angle, θ. The energy equation assuming an Ideal Adiabatic simulation [18] can be written as in (12):

$$\delta Q + c_p\, T_{in}\, dm_{in} - c_p\, T_{out}\, dm_{out} = \delta W + c_v\, d\left(mT\right), \tag{12}$$

where δQ is the thermal energy transferred into a cell of the working space and δW is the mechanical work done on the environment (positive when expanding). The non-Ideal analysis accounts for the imperfect regeneration and the pumping losses due to the friction caused by the working fluid passing throughout the engine components. The effects of the regeneration are mainly due to the convective thermal resistance between the gas and the regenerator surface, and can be modelled by using the Number of Transfer Units (NTU) method [18]. In the "loading" process, the hot working gas is pre-cooled, while flowing through the regenerator from the heater to the cooler, transferring heat to the regenerator matrix. Then, in the reverse process, the heat that was previously stored in the matrix is "discharged" and pre-heats the cold gas that flows into the heater and expansion space. The mean effective temperatures in heater (T_h) and cooler (T_k) are, respectively, lower and higher than the corresponding heat exchanger wall temperatures, heater ($T_{h,wall}$) and cooler ($T_{k,wall}$). This implies that the engine is operating between lower temperature limits than originally specified which effectively reduces the thermodynamic engine efficiency. The total heat transfer can be calculated as in (13),

$$Q = h \cdot A\left(T_{wall} - T\right), \tag{13}$$

where *h* is the heat transfer coefficient, T_{wall} is the wall temperature, and *T* the mean effective gas temperature (heater or cooler). As the temperatures are determined iteratively, Q_h and Q_k can be evaluated and the regenerator enthalpy reduction, Q_{rloss}, is quantified in terms of the regenerator effectiveness. Thus, the reduction of heat transfer in the regenerator can be quantified as a function of the regenerator effectiveness ε_r and the heat transferred to the regenerator in the ideal adiabatic conditions. The energy reduction in the regenerator can be calculated as in (14),

$$Q_{rloss} = \left(1 - \varepsilon_r\right) \cdot Q_{r,ideal}\,. \tag{14}$$

The heat for both heat exchangers is determined in (15) and (16), respectively. The less heat transfer in the regenerator leads to increases in the heats of the hot and cold sources so that, the actual heat for both heat exchangers is determined.

$$Q_k = Q_{k,ideal} + Q_{rloss} \tag{15}$$

$$Q_h = Q_{h,ideal} + Q_{rloss} \tag{16}$$

Fluid friction associated with the flow through the heat exchangers, results in a pressure drop, reducing the output power of the engine. The pressure drop (ΔP) is taken over the three heat exchangers and then, the value of the corresponding work can be achieved by integration over the complete cycle. The net engine work per cycle, *W* is thus given by Eq. (17).

$$W = \oint P\left(dV_e + dV_c\right) - W_{\Delta P}\,. \tag{17}$$

where V_e and V_c are, respectively, the expansion and compression volumes. The first term in the equation represents the ideal adiabatic work done per cycle and the second one represents the work loss per cycle, $W_{\Delta P}$, due to the pressure drops in the three heat exchangers, as presented in (18) and in (19).

$$W_{\Delta P} = \int_0^{2\pi} \delta W_{\Delta P} \tag{18}$$

$$\Leftrightarrow \quad W_{\Delta P} = \int_0^{2\pi} \left(\sum_{i=1}^{3} \Delta P_i \frac{dV_e}{d\theta} \right) \cdot d\theta \tag{19}$$

The equations that describe the Stirling engine physical model were fully presented in [19].

3.3.2. Parabolic Concentring Solar Dish

The study and design of a solar collector, its cavity receiver, require solving a mathematical model that takes into account the geometric, optical and thermal behaviour of all components. With an adequate sizing, not only the useful energy produced on the solar device will meet the energy required for the

process, but also the absorber temperature will be the needed for the operation of the Stirling engine. These systems concentrate incident solar rays to a receiver located at the focal point. The temperature in the focus of the parabola reaches high temperatures. These concentrators are assembled for rotation around two different axes to track the sun, as for maximum efficiency there is the need for incident rays to be normal to collector aperture. The absorber is located within the cavity at a distance from the aperture at which the solar image fit the entire area of the absorber. The most significant parameters of a solar concentrator are their concentration ratios. The geometric concentration ratio of a parabolic concentrator measure the extent to which the aperture area of the receiver is reduced relative to that of the concentrator dish, as given by (20),

$$C_g = \frac{A_{dish}}{A_{receiver}}, \tag{20}$$

where A_{dish} is the projected area of the concentrator, and $A_{receiver}$ is the receiver area. In practice, the geometric concentration ratio varies between 100 and 5000. The geometric concentration ratio represents the average ideal concentration of solar flux if it is distributed uniformly over the receiver aperture area. Yet, real concentrators do not produce this uniform flux. They instead produce a complex series of high and low flux levels distributed around the receiver aperture area. The flux concentration at a point is defined in terms of the optical concentration ratio, which relates the irradiation that reaches the receiver aperture, $I_{receiver}$, and the incident irradiation flux in the solar dish, I, and as in (21).

$$C_f = \frac{I_{receiver}}{I}. \tag{21}$$

If there were no losses in the reflection process, the two concentration ratios would be equal. However, in reality, C_f is always less than C_g, and a way to measure how much of the available energy that reaches the collector is transmitted to the receiver, is through the collection efficiency, as in (22),

$$\eta_{collection} = \frac{C_f}{C_g} = \frac{I_{receiver}}{I} \cdot \frac{A_{receiver}}{A_{dish}}. \tag{22}$$

Figure 2 shows the cross section of a parabolic dish concentrator. The parabolic surface has the property to reflect all the parallel beam rays to the optical axis of the mirror (i.e. axis connecting point *O* to the Focus in Figure 2), into the Focus point.

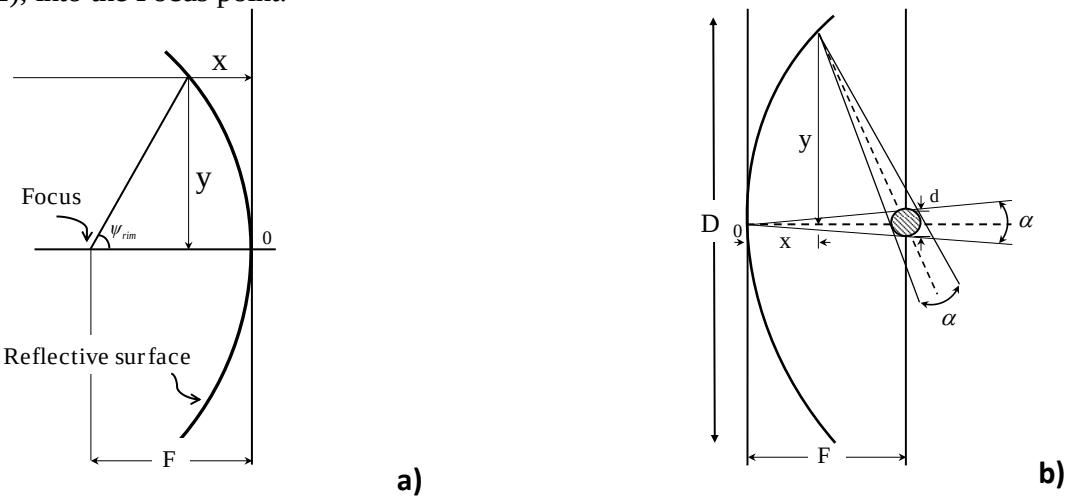

Fig. 2. ***a)*** *Geometric scheme of the parabolic profile Schematic layout of solar-powered Stirling engine for micro-cogeneration;* ***b)*** *Scheme of parabolic profile taking into account the angle of incidence.*

A parabola is a curve generated by the intersection of a right circular cone and a plane parallel to an element of the curve. Therefore, it is possible to obtain the geometric relationships, for which the Cartesian coordinates describe the curve of the focal distance of the parabola.

The design and the geometry of this type of collector can be determined by two parameters, the rim angle, ψ, and the aperture diameter, D_{dish} of the dish. The rim angle is the angle measured at the focus from the axis to the rim where the paraboloid is truncated. A paraboloid with a very small rim angle has

very little curvature, and the focal point and the receiver must be placed far from the concentrator surface. Paraboloids with rim angles less than 50 degrees are used when the reflected radiation passes into a cavity receiver, whereas paraboloids with larger rim angles are best suited for external receivers. Dish/Stirling systems have rim angles less than 50 degrees. In this study, a ψ_{rim} equal to 45º was considered. The focal distance, F, is used to determine the aperture ratio $N = D_{dish}/F$. There is a relationship between the focal length, the dish diameter and the rim angle, as presented in (23),

$$F = \frac{D_{dish}}{4\tan(\psi_{rim}/2)}. \tag{23}$$

Once the rim angle and aperture diameter of the parabolic dish are established, the focal distance can be calculated, and with that, the geometry of the concentrator is fully defined. Once the geometry of the concentrator is defined, the aperture diameter of the cavity, d_{ap}, is equal to the width of the solar image produced in the focal plane, wn, as in (24),

$$wn = 2d_{sf}\tan\left(\frac{\alpha}{2}\right)\Big/\cos\psi_{rim}, \tag{24}$$

where ψ_{rim} is the rim angle, d_{sf} is the distance from the concentrator surface to the focal point of the aperture and α is the incident angle. Beam rays do not focus on the surface perfectly parallel to each other, being necessary to quantify the incidence angle, α, as in Figure 2b). The irradiation incident on the receiver can be calculated according to equation (25), proposed by [20],

$$I_{receiver} = \frac{4I\rho}{2\tan\left(\frac{\alpha}{2}\right)^2}\left[1-\left(\frac{16-N^2}{16+N^2}\right)^2\right], \tag{25}$$

where ρ is the reflectivity. Equation shows that the irradiation that reaches the receiver ($I_{receiver}$) is not related to the individual values of dish diameter or focal length, but the aperture ratio of N. The highest value of $I_{receiver}$ is found in the centre of the solar image in the focal plane and its value decreases as we move away from this central point. Figure 3a) shows the dependence between the amount of irradiation and the position on the focal plane for different values of N, where the abscissa axis represents r/d, where r is the distance between the point focal plane and considered the centre of the solar image, and d is equal to the diameter of the solar image. The axis of ordinates shows values of the dimensionless $\left[1-\left(\frac{16-N^2}{16+N^2}\right)^2\right]$ that for $r/d > 0.5$ decreases as in the Figure 3a). This curves were obtained through a data fit, based on the work presented by [20]. Because real concentrators do not produce uniform flux, but instead they produce series of high and low flux levels distributed around the receiver aperture area, a mean value for the irradiation at the receiver should be calculated. In this sense, an average value for the irradiation is calculated, $\bar{I}_{receiver}$, weighted by the concentric areas, A_i, for each irradiation value, as shown its representation in Figure 3b), where the points in the plane (*xy*) represent the points of the focal plane (receiver aperture). Thus, the irradiation values for each of the annular regions are obtained as in (26).

$$\bar{I}_{rec} = \frac{\sum_{1}^{i} I_{receiver,i} * A_i}{A_{receiver}} \tag{26}$$

The same procedure was adopted to calculate the average temperature at the receiver. The average temperature at the receiver in the focal plane, $\bar{T}_{receiver}$, can be calculated according to (27),

$$\bar{T}^4_{receiver} - T^4_{amb} \cong \frac{4I\rho}{2\tan\left(\frac{\alpha}{2}\right)^2}\left[1-\left(\frac{16-N^2}{16+N^2}\right)^2\right]\frac{1}{\sigma}, \tag{27}$$

where T_{amb} is the environment temperature and σ is the Stefan-Boltzmann constant, assumed to be 5.670E-08 W/m^{2}K^4.

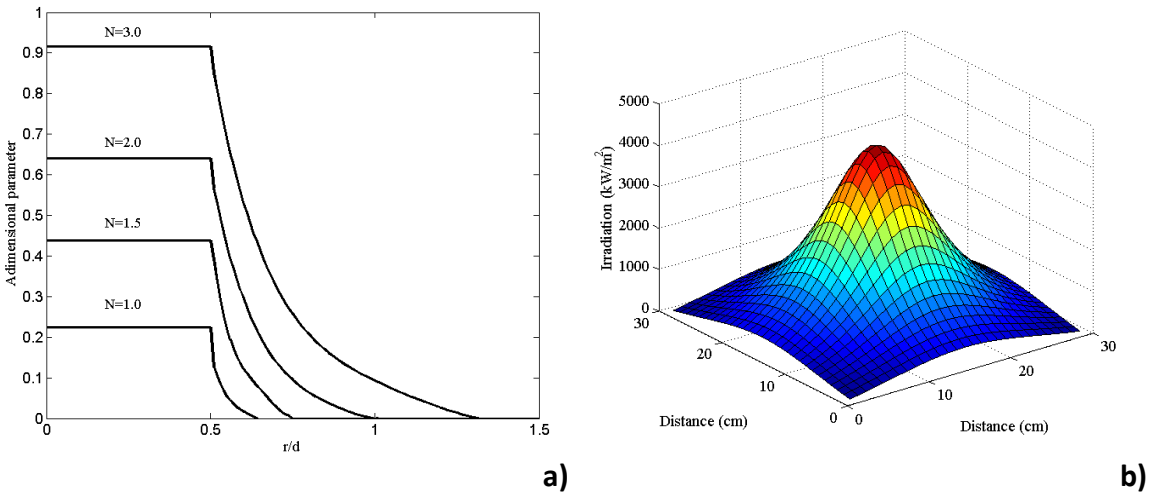

Fig. 3: a) Variation of irradiation at the receiver as a function of the position at the focal plane for different values of aperture ratio; b) Irradiation distribution in the focal plane.

The incident heat flux on the collector dish can be calculated as a function of the incident irradiation flux in the solar dish and the parabolic dish area, as in (28),

$$Q_{collector} = I \cdot A_{dish}. \tag{28}$$

The heat which will be available to the Stirling engine contained in the receiver cavity, without counting losses, can be calculated as a function of the average value for the irradiation and the receiver area, as in (29),

$$Q_{receiver} = \bar{I}_{receiver} \cdot A_{receiver}. \tag{29}$$

It is also important the fact that part of the energy that enters in the receiver is returned to the environment due to emission of the receiver itself through the opening of the cavity. The heat losses due to the surface emissivity, ε, can be calculated as a function of Stefan-Boltzmann constant, the receiver area, the average temperature at the receiver and the environment temperature, as in (30).

$$Q_{collector\_losses} = \varepsilon \sigma A_{receiver} \left(\bar{T}^4_{receiver} - T^4_{\text{amb}} \right) \tag{30}$$

Some authors [20] assume that there is a phenomenon of "trapping" of sun beams in the cavity, and so, it is plausible to assume that the receiver behaves as a black body, where the emissivity can be assumed to be 1. For simulation purposes, some assumptions were made. A constant rim angle of 45 degrees, an incidence angle of 23 degrees and the receiver aperture diameter of 16 cm were assumed based on the geometrical characteristics of the *Eurodish* Stirling system. Other optical features from the *Eurodish*-Stirling system were considered, namely, the reflectivity of 94%. Also, a constant input for the direct solar irradiation in collector was assumed to be $I = 900\, Wm^{-2}$.

3.4. Non-linear Constraints

Several inequality constraints were formulated in order to give physical significance to the mathematical model. The definition of these constraints aims bounding some of the variables according to their feasible limits in the system operation. Considering the applicability of the system, the power production was restricted to a maximum of 5 kW. In view of the data from the market, a constraint bounding the heat-to-power ratio, λ, was also included into the model. It is well known from the literature that the systems available on the market have an electric power size ranging from 1 kW to 9 kW and a corresponding thermal power size from 5 kW to 25 kW. Considering the temperature evolution, the temperature of the working gas at the cooler, T_k was also constrained. Regarding the costs of each component, inequality constraints were defined in order to guarantee the relative share in terms of costs for each system component, by assuming a respectively percentage in the total cost of the power plant, for instance, the regenerator cost should represent, at least, 25% of the total cost of the CHP system. Plus, Primary Energy Savings (PES) was also include in the model as an inequality constraint in order to guarantee that the system may be classified as high efficient CHP power plant, which for micro-scale application requires that its value should be positive (PES>0) [21].

3.5. Decision Variables

Defining the decision variables is in fact one of the hardest and/or most crucial steps in formulating an optimization problem. Based on preliminary tests to the physical model [22,23], eight explicit decision variables were defined in the numerical model. The decision variables selected were the mean pressure (P_{mean}); the cylinders swept volumes (V_{eng}); the internal diameter of heater ($d_{int,h}$) and cooler ($d_{int,k}$) tubes, the porosity of regenerator matrix (Φ) and the diameter of the matrix wire (d_{wire}); the solar collector dish diameter (d_{dish}); and the mean effective gas temperature in the heater tubes, (T_h). Upper and lower bounds were selected for these decision variables, considering their significance in the model. The values for each upper and lower limit were also defined: $5 \le P_{mean} \le 80$, $70 \le V_{eng} \le 155$, $1 \le d_{\mathrm{int},h} \le 5$, $1 \le d_{\mathrm{int},k} \le 5$, $0.3 \le \Phi_{r\_matrix} \le 0.9$, $0.2 \le d_{wire} \le 0.6$, $6.0 \le d_{dish} \le 12.0$ and $725 \le T_h \le 900$.

3.6. Numerical Solution

Concerning the complexity of the physical system, the optimization problem was solved using the Pattern Search (PS) routine in the MatLab® optimisation toolbox. Generalized Pattern Search (GPS) algorithms are derivative free methods for the optimization problems, herein explained [24]. The method is initiated with a "trial step" considering the convergence tolerance, the length of search step and the initial direction. Considering that the poll option controls how the algorithm vote the mesh points at each iteration, the simulation was carried out considering the complete poll 'on' in order to choose the point with the best objective function value by checking all the points in the mesh at each iteration. The poll method chosen was the *Positive basis 2N* Generalized Pattern Search algorithm. The search method was defined as the MADSPositiveBasis2N. The maximum number of functions evaluation was defined as 20000. This method requires a feasible initial point to start the iterative process. In this study, the initial point was assumed to be: P_{mean} = 30 bar, V_{eng} = 125 cm^3, $d_{\mathrm{int},h} = d_{\mathrm{int},k}$ =3.0 mm, Φ_{r_matrix} = 0.7, d_{wire} =0.3 mm, T_h = 750 K and d_{dish} =8.0 m. This initial point was obtained by a previous analysis of the physical system. When employing the optimization model, several script files were created to define the equations that describe the physical system and the cost equations, which depend on the most important physical parameters for each of the system components. It was also required to define the nonlinear constraints as well as the simple bounds of the decision variables (upper and lower bounds). The bounds in the variables guarantee that the optimum solution is within the technical operating capability of the plant. The main routine, where the algorithm parameters were defined, integrates all the scripts in order to solve the optimization problem.

5. Results and Discussion

The process of the thermal-economic optimization included several tests in order to delineate the most appropriate assumptions and constants in the model. Those tests include the consideration of different combinations of decision variables, working fluids, numerical methods and respective parameters as previously presented [19,21,23].

The simulations were run considering a constant rotation speed of 1500 rpm considering the helium as the working fluids. After convergence was achieved (four iterations and 4206 objective function evaluations), the optimal values for the objective function, decision variables and others thermodynamic and economic variables were obtained. The optimal solutions were obtained, no constraint was violated, the convergence tolerances were respected and the optimization terminated because the objective function was non-decreasing in feasible directions and the solution was within the value of the function tolerance. Table 1 presents the optimal annual costs and revenues from the CHP system operation. Results depicts that it is possible to obtain a positive profit from the system operation. The most predominant costs are the investment costs to acquire the system, whereas, the highest revenue came from the income from the avoided cost of separate heat generation. Arising from the fact that there is no need to have a separate system to produce the total heating demand, the economic benefit from that avoided cost was also accounted, representing a revenue of 1327 €/year. Also, the revenues from selling the produced electricity to the grid represent a great economic benefit. Results shows that for a base case scenario considering an electricity FIT of 0.12 €/kWh, it is possible to achieve an annual revenue above 1315 €/year if all the electricity generated is sold to the grid.

Stirling engine technology is characterized for long periods without need of maintenance intervention. Considering the results, the maintenance cost represents about 7% of the total annual costs of system operation and the annualized investment costs correspond to the highest charge.

Table 1. Optimal annual costs and incomes of the thermal power system

Annual Costs and Revenues, €/*year*	
Capital Investment Cost, C_{inv}	(2333)
Maintenance Costs, C_m	(164)
Revenue from equipment residual value, Rev_{res}	366
Revenue from selling electricity to the grid, Rev_{sell}	1315
Revenue from CES bonification, Rev_{ces}	117
Avoided cost from separate heat generation, $C_{avoided}$	1327
Annual worth of the CHP system, *AW*	**627**

Considering the objective function defined for this optimization problem, it may be concluded that applying thermal-economic optimization to the system allows obtaining the best economic output and, at same time optimize the physical system. The optimal values for the eight decision variables are presented in Table 2.

Table 2. Optimum values of the eight decision variables

Decision Variables	
P_{mean}, [bar]	53.0
V_{eng}, [cm^3]	158
$d_{inner,h}$, [mm]	1.50
$d_{inner,k}$, [mm]	2.74
Φ_{matrix},[-]	0.69
d_{wire}, [mm]	0.47
T_h, [K]	849
d_{dish}, [m]	7.41

Therefore, this corresponds to a thermal plant operating at a mean pressure of 53 bar, considering cylinders with a 158 cm^3 of capacity, the heater tubes with 1.50 mm for the internal diameter and the cooler tubes with 2.74 mm of internal diameter. The tubular regenerator should contain a wired matrix with a porosity of 0.687 and the with a wire diameter of 0.47 mm. The effective temperature of the gas inside the heater tubes reaches the 849 K. The optimal solar collector diameter corresponds to 7.41 m. Although the mean operational pressure is one of the physical parameters in the engine bulk purchase cost equation, the increase in the component cost is lower than the gains that are obtained in terms of power produced by the system, that somehow are intended to be maximized. The performance criteria for the optimal solutions are presented in Table 3. The results disclose similar values for the electrical and thermal powers when comparing the results with the optimal solution from the eight decision variables simulation. The optimal solution, discloses a thermal plant able to produce 3.65 kW of electrical power and 11.1 kW of thermal power. This output represents a heat-to-power ratio of 3.0, which is a value within the range for current commercial models available. In terms of performance, it was obtained an electrical efficiency of 26.2% and a total efficiency (in cogeneration mode) of 98%.

Table 3. Optimum values of thermal system performance

Performance Criteria	
Thermal Power, [kW]	11.1
Electrical Power, [kW]	3.65
Electrical Efficiency, [%]	26.2
Total Efficiency, [%]	98.1
Solar collector Efficiency [%]	94.9
PES [%]	34.8
CES [%]	27.6

Once the system uses a total renewable energy source, environmental benefits arise from the system operation. In fact, this system allows a considerable primary energy saving rate and a reduction of carbon emissions. Economic indexes were also calculated and results shown that the investment can be recovered over a period of 9 years and approximately 11 months. The Internal Rate of Return obtained was of 8%, which suggests that the investment on the micro-CHP system with these performance characteristics is still economically attractive, once the interest rate was assumed to be 7%. Results disclosed a positive Net Present Value of the 1697 € for a 20 years lifetime project.

Conclusions

In this paper, a thermal-economic optimization model of a micro-cogeneration system based on a Stirling engine with a parabolic solar collector technology is numerically modelled. A derivative free algorithm was chosen to solve the optimization model, and simulations were carried out to obtain the maximum profit of the small cogeneration system. The implemented mathematical model reached an optimal solution disclosing a positive annual worth (627 €/years) for the best physical configuration of the system. The best configuration depicts a cogeneration system able to deliver 3.65 kW of electrical power and 11.06 kW of thermal power to fulfil the base heating load of a residential building. As expected, the research shows that the most dominant cost is the purchase investment cost of the system. This outcome proves that one of the most drawbacks of renewable micro-CHP systems lies on high costs and large investment recovery periods. Another important issues, is that improvements should be performed to introduce the energy storage in the model in order to overcome the problems with the energy source intermittence. One of the most relevant aspects of this works is the cost estimation of the Stirling engine components based on the size, quality and physical parameters.

Regarding the optimization algorithm, the computational time is relatively high (i.e. four hours until getting the convergence) probably due to the complexity of physical model. A more detailed sensitivity analysis for the different parameters of the optimization method and numerical model should be carried out in order to better confirm its accuracy in finding the solution of this optimization problem. Also, different numerical methods should be tested. Tests with evolutionary algorithms are now being run.

Acknowledges

The authors are grateful for the support provided by FCT national funds under the Strategic Project PEst2015-2020, with the reference: UID/CEC/00319/2013.

References

[1] Kong XQ, Wang RZ, Huang XH. Energy efficiency and economic feasibility of CCHP driven by stirling engine. Energy Convers Manag 2004;45:1433–42. doi:10.1016/j.enconman.2003.09.009.

[2] Aliabadi A a., Thomson MJ, Wallace JS, Tzanetakis T, Lamont W, Di Carlo J. Efficiency and Emissions Measurement of a Stirling-Engine-Based Residential Microcogeneration System Run on Diesel and Biodiesel. Energy & Fuels 2009;23:1032–9. doi:10.1021/ef800778g.

[3] Shazly JH, Hafez AZ, El Shenawy ET, Eteiba MB. Simulation, design and thermal analysis of a solar Stirling engine using MATLAB. Energy Convers Manag 2014;79:626–39. doi:10.1016/j.enconman.2014.01.001.

[4] Kongtragool B, Wongwises S. Thermodynamic analysis of a Stirling engine including dead volumes of hot space, cold space and regenerator. Renew Energy 2006;31:345–59. doi:10.1016/j.renene.2005.03.012.
[5] Rogdakis ED, Antonakos GD, Koronaki IP. Thermodynamic analysis and experimental investigation of a Solo V161 Stirling cogeneration unit. Energy 2012;45:503–11. doi:10.1016/j.energy.2012.03.012.
[6] Ferreira ACM, Nunes ML, Martins LASB, Teixeira. A Review of Stirling Engine Technologies applied to micro-Cogeneration Systems. In: Desideri U, Manfrida G, Sciubba E, editors. ECOS 2012 - 25th Int. Conf. Effic. Cost, Optim. Simul. Environ. Impact Energy Syst., vol. I, Perugia, Italy: 2012, p. 1–11.
[7] Kongtragool B, Wongwises S. A review of Solar-power Stirling engines and low temperature differential Stirling engines. Renew Sustain Energy Rev 2003;7:131–54. doi:10.1016/S1364-0321(02)00053-9.
[8] Kaushik S., Kumar S. Finite time thermodynamic analysis of endoreversible Stirling heat engine with regenerative losses. Energy 2000;25:989–1003. doi:10.1016/S0360-5442(00)00023-2.
[9] Ust Y, Sahin B, Kodal A. Optimization of a dual cycle cogeneration system based on a new exergetic performance criterion. Appl Energy 2007;84:1079–91. doi:10.1016/j.apenergy.2007.04.004.
[10] Boucher J, Lanzetta F, Nika P. Optimization of a dual free piston Stirling engine. Appl Therm Eng 2007;27:802–11. doi:10.1016/j.applthermaleng.2006.10.021.
[11] Nepveu F, Ferriere A, Bataille F. Thermal model of a dish/Stirling systems. Sol Energy 2009;83:81–9. doi:10.1016/j.solener.2008.07.008.
[12] Asnaghi A, Ladjevardi SM, Saleh Izadkhast P, Kashani a. H. Thermodynamics Performance Analysis of Solar Stirling Engines. ISRN Renew Energy 2012;2012:1–14. doi:10.5402/2012/321923.
[13] Ahmadi MH, Sayyaadi H, Mohammadi AH, Barranco-Jimenez M a. Thermo-economic multi-objective optimization of solar dish-Stirling engine by implementing evolutionary algorithm. Energy Convers Manag 2013;73:370–80. doi:10.1016/j.enconman.2013.05.031.
[14] Konrad C, Obé E, Frey H. Distributed generation potential in the German residential sector. Cogener On-Site Power Rev 2009:59–65.
[15] Öberg R, Olsson F, Palsson M. Demonstration Stirling Engine based Micro-CHP with ultra-low emissions. Nordenskiöldsgatan, Sweden: 2004.
[16] Marechal F, Palazzi F, Godat J, Favrat D. Thermo-Economic Modelling and Optimisation of Fuel Cell Systems. Fuel Cells 2005;5:5–24. doi:10.1002/fuce.200400055.
[17] GmbH SS. ProEcoPolyNet Fact Sheet "SOLO Stirling 161" (Brochure) 2007:1–4.
[18] Ferreira AC, Teixeira S, Ferreira C, Teixeira J, Nunes ML, Martins LB. Thermal-Economic Modeling of a Micro-CHP Unit Based on a Stirling Engine. In: ASME, editor. Vol. 6A Energy, San Diego, California, USA: ASME; 2013, p. V06AT07A036. doi:10.1115/IMECE2013-65126.
[19] Ferreira AC, Nunes ML, Martins LB, Teixeira SF. Thermal Analysis and Cost Estimation of Stirling Cycle Engine. World Sci Eng Acad Soc Trans Power Syst 2014:11 pgs.
[20] Fujii I. From solar energy to mechanical power. 1st ed. Chur ; New York : Harwood Academic Publishers; 1990.
[21] Ferreira AC, Nunes M, Martins L, Teixeira S. Maximum Profit of a Cogeneration System based on Stirling Thermodynamic Cycle. 2014 14th Int. Conf. Comput. Sci. Its Appl. (ICCSA 2014), IEEE Computer Society; 2014, p. 156–60. doi:10.1109/ICCSA.2014.36.
[22] Ferreira AC, Teixeira S, Nunes ML, Martins LB. Numerical Study of Regenerator Configuration in the Design of a Stirling Engine. In: ASME (Ed.), editor. Proc. ASME 2014 Int. Mech. Eng. Congr. Expo. IMECE2014, vol. Volume 6A:, Montereal, Canada: ASME; 2014, p. pp. V06AT07A021; 10 pages. doi:10.1115/IMECE2014-38529.
[23] Ferreira ACM, Nunes ML, Martins LB, Teixeira SF. Analysis of the geometrical parameters of thermal components in a stirling engine. 11th World Congr. Comput. Mech. WCCM 2014, 5th Eur. Conf. Comput. Mech. ECCM 2014 6th Eur. Conf. Comput. Fluid Dyn. ECFD 2014, International Center for Numerical Methods in Engineering; 2014, p. 3734–45.
[24] Lewis RM, Shepherd A, Torczon V. Implementing Generating Set Search Methods for Linearly Constrained Minimization. SIAM J Sci Comput 2007;29:2507–30. doi:10.1137/050635432.